

# Probing the critical exponent of the superfluid fraction in a strongly interacting Fermi gas

Hui Hu and Xia-Ji Liu\*

Centre for Atom Optics and Ultrafast Spectroscopy, Swinburne University of Technology, Melbourne 3122, Australia

(Received 7 October 2013; published 26 November 2013)

We theoretically investigate the critical behavior of a second-sound mode in a harmonically trapped ultracold atomic Fermi gas with resonant interactions. Near the superfluid phase transition with critical temperature  $T_c$ , the frequency or the sound velocity of the second-sound mode crucially depends on the critical exponent  $\beta$  of the superfluid fraction. In an isotropic harmonic trap, we predict that the mode frequency diverges like  $(1 - T/T_c)^{\beta-1/2}$  when  $\beta < 1/2$ . In a highly elongated trap, the speed of the second sound reduces by a factor of  $1/\sqrt{2\beta + 1}$  from that in a homogeneous three-dimensional superfluid. Our prediction could readily be tested by measurements of second-sound wave propagation in a setup, such as that exploited by Sidorenkov *et al.* [Nature (London) **498**, 78 (2013)] for resonantly interacting lithium-6 atoms, once the experimental precision is improved.

DOI: 10.1103/PhysRevA.88.053635

PACS number(s): 03.75.Kk, 03.75.Ss, 67.25.D–

## I. INTRODUCTION

Superfluidity, a remarkable state of matter in which particle flows with zero resistance, is a ubiquitous quantum phenomenon occurring in diverse systems, ranging from liquid helium, high-temperature superconductors, to neutron stars [1,2]. Whereas, at zero temperature, all the particles in the system participate in the superfluid motion, at finite temperatures because of thermal excitations, only a portion of particles—named the superfluid fraction—behaves in such a way. The remaining particles comprise a normal fluid component that behaves like an ordinary fluid [3,4]. To characterize superfluidity, it is, therefore, crucial to understand the superfluid fraction, which, unfortunately, is notoriously difficult to calculate microscopically for strongly interacting quantum systems, especially near the superfluid phase transition. In this respect, the recently realized ultracold atomic Fermi gases with controllable interatomic interactions and external harmonic trapping potentials [5,6], known as a new type of strongly interacting superfluid, provide unique opportunities for exploring superfluidity and for understanding the superfluid fraction in the strongly interacting regime. In this paper, we propose that the critical behavior of the superfluid fraction of a resonantly interacting atomic Fermi gas at unitarity (where atoms occupying unlike spin states interact with an infinitely large scattering length) could be well characterized through the measurement of second-sound propagation.

Second sound as well as first sound are the coupled oscillations of the superfluid and normal fluid components at finite temperatures [3,4]. In contrast to first sound, which is an in-phase oscillation of the two components (i.e., density oscillation), second sound is an out-of-phase oscillation (i.e., temperature or entropy wave) and depends very sensitively on the superfluid fraction. Therefore, it presents, arguably, the most dramatic manifestation of superfluidity. Indeed, in superfluid helium, the accurate determination of the superfluid fraction, slightly below the  $\lambda$  point, is provided by the

measurement of second sound [7]. Very recently, for a resonantly interacting Fermi gas of lithium-6 atoms confined in highly elongated harmonic traps, the superfluid fraction was qualitatively extracted from the measurement of the second-sound velocity along the weakly confined axial direction as reported by Sidorenkov *et al.* [8]. This milestone experiment already imposes a grand challenge since the theoretical predictions for the temperature dependence of the superfluid fraction in the unitary limit are rather incomplete [9–12]. Our proposal, together with future second-sound measurements with better precision in such ultracold atomic systems, allows an accurate determination of the critical behavior of the superfluid fraction just below the superfluid phase transition.

Our main results are briefly summarized as follows. We consider both isotropic and highly elongated harmonic traps. The latter situation is exactly the setup exploited in the current experiment [8]. For isotropic traps, we find that, slightly below the superfluid transition temperature  $T_c$ , the mode frequency of the second sound diverges as  $(1 - T/T_c)^{\beta-1/2}$  if the critical exponent of the superfluid fraction is  $\beta < 1/2$ . Whereas, for highly elongated traps, the speed of the second sound along the weakly confined direction reduces by a factor of  $1/\sqrt{2\beta + 1}$  from that in a three-dimensional free space. In both cases, the sensitive dependence of the second-sound mode on the critical exponent leads to an accurate calibration of  $\beta$ .

## II. TWO-FLUID HYDRODYNAMICS

First and second sounds are well described by the equations of two-fluid hydrodynamics first derived by Landau [4]. As discussed in the previous papers [9,13,14], in the dissipationless regime, the solutions of these hydrodynamic equations with frequency  $\omega$  at temperature  $T$  can be derived by minimizing a variational action, which, in the terms of displacement fields  $\mathbf{u}_s(\mathbf{r})$  and  $\mathbf{u}_n(\mathbf{r})$ , is given by,

$$S = \frac{1}{2} \int d\mathbf{r} \left[ \omega^2 (\rho_{s0} \mathbf{u}_s^2 + \rho_{n0} \mathbf{u}_n^2) - \frac{1}{\rho_0} \left( \frac{\partial P}{\partial \rho} \right)_{\bar{s}} (\delta\rho)^2 - 2\rho_0 \left( \frac{\partial T}{\partial \rho} \right)_{\bar{s}} \delta\rho \delta\bar{s} - \rho_0 \left( \frac{\partial T}{\partial \bar{s}} \right)_{\rho} (\delta\bar{s})^2 \right]. \quad (1)$$

\*xiajiliu@swin.edu.au

Here,  $\rho_s(\mathbf{r})$  and  $\rho_n(\mathbf{r})$  are the superfluid and normal fluid densities for a gas with total mass density  $\rho(\mathbf{r}) \equiv mn = \rho_s + \rho_n$ .  $P(\mathbf{r})$  is the local pressure of the gas, and  $\bar{s}(\mathbf{r}) = s/\rho$  is the entropy per unit mass.  $\delta\rho(\mathbf{r}) = -\nabla \cdot [\rho_{s0}\mathbf{u}_s + \rho_{n0}\mathbf{u}_n]$  and  $\delta\bar{s}(\mathbf{r}) = -\mathbf{u}_n \cdot \nabla\bar{s}_0 + (\bar{s}_0/\rho_0)\nabla \cdot [\rho_{s0}(\mathbf{u}_s - \mathbf{u}_n)]$  are the density and entropy fluctuations, respectively. The displacement fields are related to the superfluid and normal velocity fields by  $d\mathbf{u}_s/dt = \mathbf{v}_s$  and  $d\mathbf{u}_n/dt = \mathbf{v}_n$ . The effect of the external harmonic trapping potential  $V_T(\mathbf{r}) = m\omega_T^2 r_\perp^2/2 + m\omega_z^2 z^2/2$  enters Eq. (1) through the position-dependent equilibrium thermodynamic functions, which we have indicated by the subscript “0”. For a resonantly interacting Fermi gas, all these thermodynamic functions—except for the superfluid density—are known to certain precision, owing to the recent experimental analysis of the homogeneous equation of state performed by the Massachusetts Institute of Technology (MIT) team [15] by using the universality relations satisfied by the unitary Fermi gas [16,17] and the parallel theoretical progress [18,19]. Throughout the paper, we calculate the trapped density profile and thermodynamic functions based on the smoothed experimental MIT data [15] and the local density approximation (LDA), which amount to setting a local chemical potential  $\mu(\mathbf{r}) = \mu - V_T(\mathbf{r})$ , where  $\mu$  is the chemical potential at the trap center.

In the absence of the coupling term between density and entropy fluctuations [i.e.,  $\rho_0(\partial T/\partial\rho)_{\bar{s}} = 0$ ], Eq. (1) admits two decoupled solutions: a pure in-phase mode with the ansatz  $\mathbf{u}_s(\mathbf{r}) = \mathbf{u}_n(\mathbf{r}) = \mathbf{u}^{(1)}(\mathbf{r})$  and a pure out-of-phase mode with  $\rho_{s0}\mathbf{u}_s^{(2)}(\mathbf{r}) + \rho_{n0}\mathbf{u}_n^{(2)}(\mathbf{r}) = 0$ , which may be referred to as the first and second sounds, respectively. These first- and second-sound modes are the exact variational solutions for pure density [ $\delta T(\mathbf{r}) = 0$ ] and pure temperature [ $\delta\rho(\mathbf{r}) = 0$ ] oscillations. When the coefficient  $\rho_0(\partial T/\partial\rho)_{\bar{s}}$  is nonzero, the first and second sounds are necessarily coupled. This coupling can conveniently be characterized by the dimensionless Landau-Placzek (LP) parameter  $\epsilon_{\text{LP}} \equiv \gamma - 1$  [20], where  $\gamma \equiv \bar{c}_p/\bar{c}_v$  is the ratio between the equilibrium specific heats per unit mass at constant pressure [ $\bar{c}_p = T(\partial\bar{s}/\partial T)_p$ ] and density [ $\bar{c}_v = T(\partial\bar{s}/\partial T)_\rho$ ]. In superfluid helium,  $\bar{c}_p \simeq \bar{c}_v$  or  $\epsilon_{\text{LP}} \simeq 0$ , implying  $\rho_0(\partial T/\partial\rho)_{\bar{s}} \simeq 0$ . Thus, the solutions of the two-fluid hydrodynamic equations for superfluid helium are described perfectly by decoupled first- and second-sound modes. For resonantly interacting atomic Fermi gases, the universality relations give rise to  $\rho_0(\partial T/\partial\rho)_{\bar{s}} = 2T/3 \neq 0$  [9]. Close to the superfluid transition temperature  $T_c \simeq 0.167T_F$ , where  $T_F$  is the Fermi temperature, we estimate, from the MIT data, that the LP parameter is about  $\epsilon_{\text{LP}} \simeq 0.4$ . Therefore, similar to superfluid liquid helium, the solutions of two-fluid equations for a unitary Fermi gas are well approximated by weakly coupled first- and second-sound modes. We note that the smallness of the LP parameter in superfluid helium and the unitary Fermi gas and, hence, the weak coupling between their first and their second modes is a general consequence of strong interactions [20]. Note also that the existence of harmonic traps will significantly reduce the sound mode coupling as we will see later. Hereafter, we focus on the second-sound mode by neglecting its coupling to the first-sound mode. In the past, the first-sound mode of a unitary Fermi gas had been studied in greater detail, both at zero temperature [21–24] and at finite temperatures [25].

### III. SECOND SOUND NEAR SUPERFLUID TRANSITION

Inserting the ansatz  $\mathbf{u}_n^{(2)}(\mathbf{r}) = -(\rho_{s0}/\rho_{n0})\mathbf{u}_s^{(2)}(\mathbf{r})$  for the second sound into Eq. (1), taking the variation with respect to  $\mathbf{u}_s^{(2)}(\mathbf{r})$ , and making use of standard thermodynamic relations, we obtain the following equation for the superfluid displacement field [14]:

$$\omega^2 \mathbf{u}_s^{(2)} = -\bar{s}_0 \nabla \cdot \left[ \frac{1}{\rho_0} \left( \frac{\partial T}{\partial \bar{s}} \right)_\rho \nabla \cdot \left( \frac{s_0 \rho_{s0}}{\rho_{n0}} \mathbf{u}_s^{(2)} \right) \right]. \quad (2)$$

As  $\delta\rho(\mathbf{r}) = 0$  for the second sound, we may also rewrite the above equation into a closed form for the temperature fluctuation  $\delta T(\mathbf{r}) = (\partial T/\partial\rho)_{\bar{s}}\delta\rho(\mathbf{r}) + (\partial T/\partial\bar{s})_\rho\delta\bar{s}(\mathbf{r}) = \rho_0^{-1}(\partial T/\partial\bar{s})_\rho \nabla \cdot [s_0 \rho_{s0} \mathbf{u}_s^{(2)}/\rho_{n0}]$ , where  $\delta\bar{s}(\mathbf{r})$  is the entropy fluctuation described below Eq. (1). This gives rise to

$$\omega^2 \delta T(\mathbf{r}) = -\frac{1}{\rho_0} \left( \frac{\partial T}{\partial \bar{s}} \right)_\rho \nabla \cdot \left[ \frac{\bar{s}_0^2 \rho_0 \rho_{s0}}{\rho_{n0}} \nabla \delta T(\mathbf{r}) \right]. \quad (3)$$

In homogeneous space, where  $\delta T(\mathbf{r}) \propto e^{i\mathbf{k}\cdot\mathbf{r}}$ , we recover the well-known result for the second-sound velocity:  $c_{2,\text{hom}}^2 = T(\bar{s}_0^2 \rho_{s0})/(\bar{c}_v \rho_{n0})$ .

In the presence of harmonic traps, it seems to be cumbersome to directly solve Eq. (3). Fortunately, near the superfluid transition, this equation could be greatly simplified as the temperature oscillation has to be restricted in a small superfluid area around the trap center, and therefore, we may safely neglect the position dependence of all thermodynamic functions—except for the superfluid density. Furthermore, close to transition, it is reasonable to assume the following critical behavior for the superfluid fraction:

$$\frac{\rho_{s0}}{\rho_{n0}}(T) \simeq \eta \left( 1 - \frac{T}{T_c} \right)^{2\beta}, \quad (4)$$

where the constant  $\eta$  and the critical exponent  $\beta$  are to be determined for a unitary Fermi gas. From the Leggett model of pairing at unitarity, it is known that the mean-field BCS wave function gives rise to  $\eta = 2$  and  $\beta = 1/2$  [26]. However, a superfluid with a two-component order parameter (and a bosonic fluctuation spectrum) generally undergoes a second-order phase transition with a superfluid density that varies as  $\rho_s \propto (T_c - T)^{2/3}$  close to the transition, independent of the interaction strength [27]. Indeed, in superfluid liquid helium, the second-sound measurement suggests that  $\eta \simeq 3.2$  and  $\beta \simeq 1/3$  [7]. In the following, we will consider these two typical sets of critical behavior for the superfluid fraction and compare the resulting prediction with the recent experimental measurement [8]. The actual values  $\eta$  and  $\beta$  are independent of each other and may be notably different from the two typical sets that we have chosen. With these considerations, we find that, within the LDA,

$$\omega^2 \delta T = -\frac{\eta k_B T_F f_s^2}{m f'_s} \nabla \cdot \left\{ \left( 1 - \frac{T}{T_c} \right)^{2\beta} \times \left[ 1 - \frac{T V_T(\mathbf{r})/k_B}{(T_c - T)(T_F f_\mu - T f'_\mu)} \right]^{2\beta} \nabla \delta T \right\}, \quad (5)$$

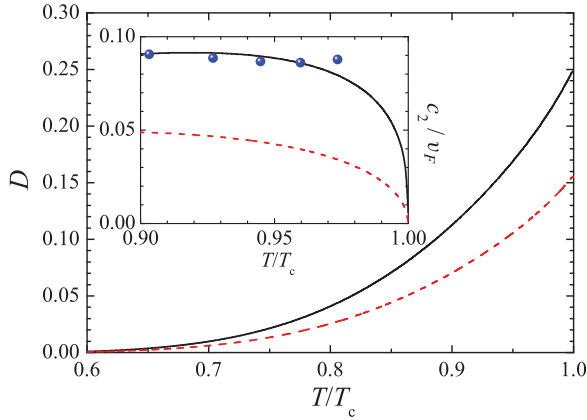


FIG. 1. (Color online) Temperature dependence of the parameter  $\mathcal{D}$  near the superfluid transition temperature  $T_c \simeq 0.167T_F$  for a strongly interacting unitary Fermi gas. We consider two types of critical behavior for the superfluid fraction  $\eta(1 - T/T_c)^{2\beta}$ : (1) superfluid helium for which  $\eta \simeq 3.2$  and  $\beta \simeq 1/3$  as shown by the black solid line, and (2) mean-field theory in which  $\eta = 2$  and  $\beta = 1/2$  as shown by the red dashed line. The inset shows the second-sound velocity of a homogeneous unitary Fermi gas  $c_{2,\text{hom}} = \sqrt{T(\bar{s}_0^2 \rho_{s0}) / (\bar{c}_v \rho_{n0})}$  in units of the Fermi velocity  $v_F = \hbar k_F / m$ , calculated using the assumed superfluid fraction Eq. (4). The blue solid circles are the theoretical predictions obtained by using the measured superfluid density, which was found to be close to that of superfluid helium [8].

where we have expressed the entropy and chemical potential of a uniform unitary Fermi gas in terms of dimensionless functions of the reduced temperature  $T/T_F$ :  $s = nk_B f_s(T/T_F)$  and  $\mu = k_B T_F f_\mu(T/T_F)$ ;  $T_F = \hbar^2 (3\pi^2 n)^{2/3} / (2mk_B)$  is the Fermi temperature at the trap center with density  $n$ , and  $f'_{s,\mu} \equiv df_{s,\mu} / d(T/T_F)$ .

It is readily seen that the superfluid area is restricted to  $r_\perp \leq R_{\perp s}$  and  $z \leq R_{zs}$ , where  $m\omega_T^2 R_{\perp s}^2 / 2 = m\omega_z^2 R_{zs}^2 / 2 = (T_c/T - 1)k_B(T_F f_\mu - T f'_\mu)$ . By introducing the scaled coordinates  $\tilde{r}_\perp = r_\perp / R_{\perp s}$  and  $\tilde{z} = z / R_{zs}$ , we may rewrite Eq. (5) into the following dimensionless form:

$$\tilde{\omega}^2 \delta T + \tilde{\nabla} \cdot [(1 - \tilde{r}_\perp^2 - \tilde{z}^2 / \lambda^2)^{2\beta} \tilde{\nabla} \delta T] = 0, \quad (6)$$

where  $\lambda \equiv \omega_T / \omega_z$  is the aspect ratio of the harmonic trap and a reduced mode frequency  $\tilde{\omega}$  is defined by

$$\omega \equiv \tilde{\omega} \sqrt{\mathcal{D}} (1 - T/T_c)^{\beta-1/2} \omega_T, \quad (7)$$

with  $\mathcal{D} = \eta(T T_F f_s^2) / [2T_c f'_s (T_F f_\mu - T f'_\mu)]$ . In Fig. 1, we show the temperature dependence of the parameter  $\mathcal{D}$  near the superfluid transition, calculated using the MIT data for the equation of state of a unitary Fermi gas [15]. It is typically at about 0.2. From Eq. (7), one may immediately realize that, for any nonzero discrete mode frequency, it would become divergent when temperature approaches the superfluid transition temperature if the critical exponent  $\beta < 1/2$ .

### A. Isotropic traps

For an isotropic harmonic trap, we may recast Eq. (6) into a one-dimensional (1D) differential equation, for example, in the sector of zero angular momentum  $l = 0$  (i.e., breathing

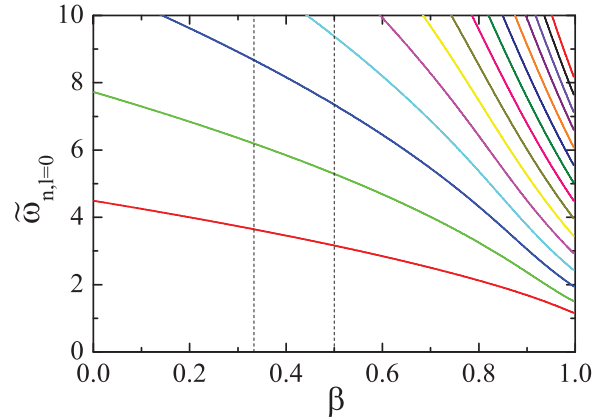


FIG. 2. (Color online) Reduced second-sound mode frequency as a function of the critical exponent  $\beta$  for an isotropically trapped unitary Fermi gas. We only consider the  $l = 0$  sector. In the cases that  $\beta$  is an integer or half-integer, the reduced frequency is known analytically. In particular, the reduced mode frequency at  $\beta = 1/2$  is given by  $\tilde{\omega}_{n,l=0} = 2\sqrt{n(n+3/2)}$ .

modes),

$$\left[ R(x) \frac{d^2}{dx^2} + P(x) \frac{d}{dx} + Q(x) \right] \delta T(x) = 0, \quad (8)$$

where  $x \equiv \tilde{r}^2 \leq 1$  and the coefficients  $R(x) = x(1-x)^{2\beta+1}$ ,  $P(x) = [3/2 - (3/2 + 2\beta)x](1-x)^{2\beta}$ , and  $Q(x) = \tilde{\omega}^2(1-x)/4$ . It can be solved numerically by using a multiseres expansion method [28]. The numerical results are reported in Fig. 2. The reduced mode frequencies decrease quickly with increasing the critical exponent  $\beta$ . When  $\beta$  is an integer or half-integer, our numerical results could be examined analytically as the solutions for the temperature fluctuation are simply polynomials and, therefore, the mode frequencies are known precisely. Indeed, for  $\beta = 1/2$  (i.e., mean-field superfluid fraction), Eq. (6) has exactly the same structure as the hydrodynamic equation that describes collective oscillations of a zero-temperature Bose condensate [29,30]. It admits analytical solutions for harmonic traps with arbitrary aspect ratios. In the case of isotropic traps, the reduced mode frequency is given by  $\tilde{\omega}_{nl} = 2\sqrt{n^2 + nl + 3n/2 + l/2}$  [29].

Now, we are able to calculate the mode frequency by using Eq. (7). The two lowest mode frequencies are shown in Fig. 3 for the superfluid-helium-like superfluid fraction (black solid lines) or mean-field-like superfluid fraction (red dashed lines). In the former case, the divergence of the mode frequency near the superfluid transition is evident as we may anticipate.

For isotropic traps, it is worth noting that the equations of two-fluid hydrodynamics can be solved fully by using a variational approach [14]. We have performed such a calculation with a mean-field superfluid fraction. The results for the lowest second-sound mode frequency are reported in Fig. 3 with blue solid circles. The good agreement between the full variational calculation and the prediction of the simplified second-sound Eq. (6) gives a reasonable justification for all the assumptions that we have made to derive Eq. (6), including neglecting the coupling between first- and second-sound modes and the ignorance of the position dependence of the thermodynamic functions used in Eq. (3).

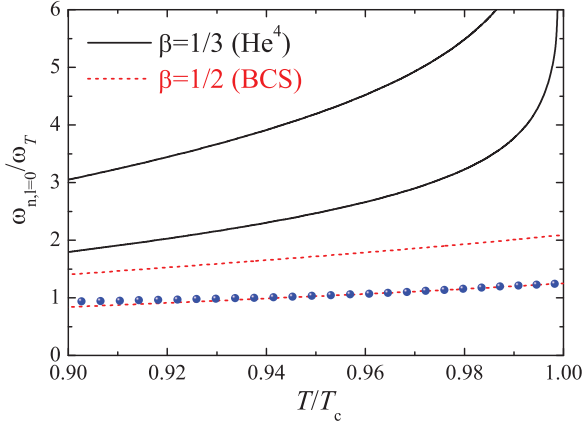


FIG. 3. (Color online) Temperature dependence of the two (lowest breathing) second-sound mode frequencies of an isotropically trapped unitary Fermi gas near the superfluid transition temperature. For a critical exponent  $\beta < 1/2$ , the mode frequency diverges at the transition. The blue solid circles are the full variational results of the two-fluid hydrodynamic equations for the lowest breathing second-sound mode.

### B. Highly elongated traps

Experimentally, a resonantly interacting atomic Fermi gas is trapped in highly elongated harmonic trapping potentials. The second sound is excited and is propagated one dimensionally along the long trap direction [8]. For such a configuration, we may assume that the temperature fluctuation has the form  $\delta T(\tilde{r}_\perp, \tilde{z}) = \delta T(\tilde{r}_\perp) e^{i\tilde{k}\tilde{z}}$ , where  $\tilde{k} \equiv kR_\perp$  is the reduced wave vector. The fluctuation field  $\delta T(\tilde{r}_\perp)$  then satisfies

$$[\tilde{\omega}^2 - \tilde{k}^2(1 - \tilde{r}_\perp^2)^{2\beta}] \delta T + \tilde{\nabla} \cdot [(1 - \tilde{r}_\perp^2)^{2\beta} \tilde{\nabla} \delta T] = 0. \quad (9)$$

For any reduced wave vector  $\tilde{k}$ , similar to the case of isotropic traps, the above equation in the sector of  $l = 0$  can be rewritten in the 1D differential form Eq. (8) by setting  $x = \tilde{r}_\perp^2$  but with new coefficients  $P(x) = [1 - (1 + 2\beta)x](1 - x)^{2\beta}$  and  $Q(x) = [\tilde{\omega}^2 - (1 - x)^{2\beta}]/4$ . It can be solved numerically following Ref. [28]. Figure 4 shows the results for  $\beta = 1/3$  and  $\beta = 1/2$ . In the latter case, our result in Fig. 4(b) agrees exactly with the earlier prediction on first-sound propagation of a zero-temperature Bose condensate in highly elongated harmonic traps [31–33] as it should be.

In Fig. 4, we observe multibranches in the spectrum, each of which corresponds to a discrete radial excitation [31,33]. The lowest branch is of particular interest as it resembles the phonon mode in free space and is the easiest mode to excite experimentally. The associated second-sound velocity is given by  $c_{2,1D} = \partial\omega/\partial k = (\partial\tilde{\omega}/\partial\tilde{k})c_{2,\text{hom}}$ . Thus, the velocity of the second sound propagated in quasi-1D geometry is reduced by a factor of  $\tilde{c} = \partial\tilde{\omega}/\partial\tilde{k}$  with respect to the bulk value  $c_{2,\text{hom}}$ . The similar quenching of first-sound velocity due to confinement was pointed out earlier for a unitary Fermi gas [32] or a Bose condensate [31]. The value of  $\tilde{c}$  may be calculated by integrating out the transverse coordinate  $\tilde{r}_\perp$  in Eq. (9):  $\tilde{c}^2 = \int d\mathbf{r}_\perp (1 - \tilde{r}_\perp^2)^{2\beta} \delta T(\tilde{r}_\perp) / \int d\mathbf{r}_\perp \delta T(\tilde{r}_\perp)$ . In the limit of long wavelength ( $\tilde{k} \rightarrow 0$ ) where the temperature fluctuation  $\delta T(\tilde{r}_\perp)$  is radially independent, we find that  $\tilde{c} = 1/\sqrt{2\beta + 1}$  in agreement with our numerical result shown in Fig. 4(c).

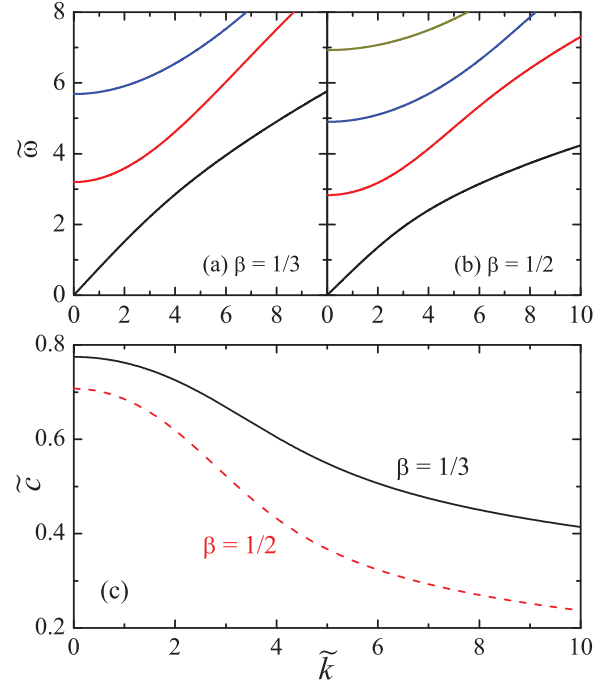


FIG. 4. (Color online) Reduced second-sound mode frequency for a unitary Fermi gas confined in highly elongated harmonic traps for the critical exponents (a)  $\beta = 1/3$  and (b)  $\beta = 1/2$ . We assume that the second sound can propagate freely along the long trap axis. In (c), we show the reduced second-sound velocity  $\tilde{c} = \partial\tilde{\omega}/\partial\tilde{k}$  for the lowest phonon modes.

In Fig. 5, we report the 1D second-sound velocity  $c_{2,\text{hom}}/\sqrt{2\beta + 1}$  by using the assumed superfluid-helium- or mean-field-like superfluid fraction Eq. (4). For comparison, we also show the experimental data extracted from Fig. 3(a) of Ref. [8]. Close to the superfluid transition (i.e.,  $T > 0.95T_c$ ), our prediction of the 1D second-sound velocity with the superfluid-helium-like superfluid fraction agrees reasonably well with the measurement. By noting that the superfluid

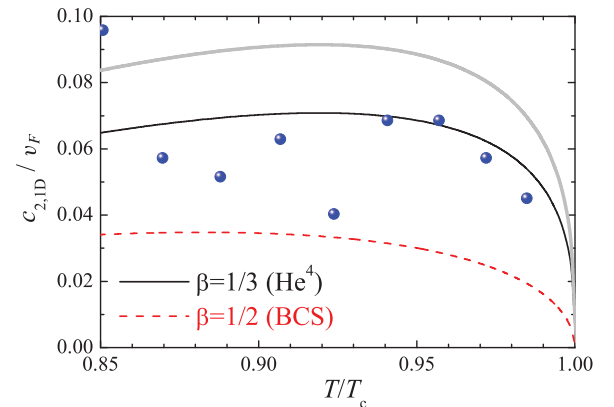


FIG. 5. (Color online) Second-sound velocity for a unitary Fermi gas confined in highly elongated harmonic traps for the critical exponent  $\beta = 1/3$  (black solid line) and  $\beta = 1/2$  (red dashed line). The blue solid circles are the experimental results extracted from Fig. 3(a) of Ref. [8] by assuming that the peak density at the trap center is unchanged close to superfluid transition. For comparison, with the gray line, we also show the bulk second-sound velocity for  $\beta = 1/3$ .

fraction of a unitary Fermi gas resembles that of superfluid helium [8], this agreement somehow is an indication of the quenched second-sound velocity. However, a quantitative experimental determination of the critical exponent  $\beta$  requires a much better precision of data.

#### IV. CONCLUSIONS

In conclusion, we have investigated, theoretically, how the second sound of a harmonically trapped unitary Fermi gas is affected by the critical exponent  $\beta$  of a superfluid fraction near the superfluid phase transition when temperature  $T$  approaches the critical temperature  $T_c$ . In an isotropic trap, the sound frequency goes like  $(1 - T/T_c)^{\beta-1/2}$  and, therefore, clearly

exhibits a divergence when  $\beta < 1/2$ . In an experimentally exploited highly elongated trap, the second-sound velocity along the long trap axis reduces by a factor of  $1/\sqrt{2\beta+1}$  with respect to its bulk value. Our prediction could be used to directly measure the critical exponent  $\beta$  in future experiments if the experimental accuracy improves.

#### ACKNOWLEDGMENTS

We thank E. Taylor, A. Griffin, L. Pitaevskii, and S. Stringari for their stimulating discussions during the early stage of this work in 2009. This work was supported by the ARC Discovery Projects (Grants No. DP0984522 and No. DP0984637) and NFRP-China (Grant No. 2011CB921502).

- 
- [1] I. M. Khalatnikov, *An Introduction to the Theory of Superfluidity* (Benjamin, New York, 1965).
- [2] P. Nozières and D. Pines, *The Theory of Quantum Liquids* (Addison-Wesley, Redwood City, CA, 1989).
- [3] L. Tisza, *C. R. Phys.* **207**, 1035 (1938).
- [4] L. D. Landau, *J. Phys. (USSR)* **5**, 71 (1941).
- [5] K. M. O'Hara, S. L. Hemmer, M. E. Gehm, S. R. Granade, and J. E. Thomas, *Science* **298**, 2179 (2002).
- [6] S. Giorgini, L. P. Pitaevskii, and S. Stringari, *Rev. Mod. Phys.* **80**, 1215 (2008).
- [7] J. G. Dash and R. D. Taylor, *Phys. Rev.* **105**, 7 (1957).
- [8] L. A. Sidorenkov, M. K. Tey, R. Grimm, Y.-H. Hou, L. Pitaevskii, and S. Stringari, *Nature (London)* **498**, 78 (2013).
- [9] E. Taylor, H. Hu, X.-J. Liu, and A. Griffin, *Phys. Rev. A* **77**, 033608 (2008).
- [10] R. Watanabe, S. Tsuchiya, and Y. Ohashi, *Phys. Rev. A* **82**, 043630 (2010).
- [11] L. Salasnich, *Phys. Rev. A* **82**, 063619 (2010).
- [12] G. Baym and C. J. Pethick, *Phys. Rev. A* **88**, 043631 (2013).
- [13] E. Taylor and A. Griffin, *Phys. Rev. A* **72**, 053630 (2005).
- [14] E. Taylor, H. Hu, X.-J. Liu, L. P. Pitaevskii, A. Griffin, and S. Stringari, *Phys. Rev. A* **80**, 053601 (2009).
- [15] M. J. H. Ku, A. T. Sommer, L. W. Cheuk, and M. W. Zwierlein, *Science* **335**, 563 (2012).
- [16] T.-L. Ho, *Phys. Rev. Lett.* **92**, 090402 (2004).
- [17] H. Hu, P. D. Drummond, and X.-J. Liu, *Nat. Phys.* **3**, 469 (2007).
- [18] H. Hu, X.-J. Liu, and P. D. Drummond, *Phys. Rev. A* **77**, 061605(R) (2008).
- [19] H. Hu, X.-J. Liu, and P. D. Drummond, *New J. Phys.* **12**, 063038 (2010).
- [20] H. Hu, E. Taylor, X.-J. Liu, S. Stringari, and A. Griffin, *New J. Phys.* **12**, 043040 (2010).
- [21] S. Stringari, *Europhys. Lett.* **65**, 749 (2004).
- [22] H. Hu, A. Minguzzi, X.-J. Liu, and M. P. Tosi, *Phys. Rev. Lett.* **93**, 190403 (2004).
- [23] A. Altmeyer, S. Riedl, C. Kohstall, M. J. Wright, R. Geursen, M. Bartenstein, C. Chin, J. Hecker Denschlag, and R. Grimm, *Phys. Rev. Lett.* **98**, 040401 (2007).
- [24] J. Joseph, B. Clancy, L. Luo, J. Kinast, A. Turlapov, and J. E. Thomas, *Phys. Rev. Lett.* **98**, 170401 (2007).
- [25] M. K. Tey, L. A. Sidorenkov, E. R. Sánchez Guajardo, R. Grimm, M. J. H. Ku, M. W. Zwierlein, Y.-H. Hou, L. Pitaevskii, and S. Stringari, *Phys. Rev. Lett.* **110**, 055303 (2013).
- [26] A. J. Leggett, *Quantum Liquids: Bose Condensation and Cooper Pairing in Condensed-Matter Systems* (Oxford University Press, Oxford, 2006), Chap. 8.
- [27] E. M. Lifshitz and L. P. Pitaevskii, *Statistical Physics, Part 2* (Butterworth-Heinemann, Oxford, 2002), Sec. 28.
- [28] X.-J. Liu, H. Hu, and P. D. Drummond, *Phys. Rev. A* **77**, 013622 (2008).
- [29] S. Stringari, *Phys. Rev. Lett.* **77**, 2360 (1996).
- [30] M. Fliesser, A. Csordás, P. Szépfalussy, and R. Graham, *Phys. Rev. A* **56**, R2533 (1997).
- [31] E. Zaremba, *Phys. Rev. A* **57**, 518 (1998).
- [32] P. Capuzzi, P. Vignolo, F. Federici, and M. P. Tosi, *Phys. Rev. A* **73**, 021603(R) (2006).
- [33] T. K. Ghosh and K. Machida, *Phys. Rev. A* **73**, 013613 (2006).